



GLOBAL JOURNAL OF HUMAN-SOCIAL SCIENCE: B
GEOGRAPHY, GEO-SCIENCES, ENVIRONMENTAL SCIENCE & DISASTER
MANAGEMENT

Volume 21 Issue 3 Version 1.0 Year 2021

Type: Double Blind Peer Reviewed International Research Journal

Publisher: Global Journals

Online ISSN: 2249-460X & Print ISSN: 0975-587X

Influence of Leaf Area Index on the Heat Index of a Tropic Urban Park

By Jonathan Willian Zangeski Novais, Danielle Da Silva Batista, Renata Luisa Ferreira, Roberta Daniela de Souza, Thiago Fernandes & Carlo Ralph De Musis

Universidade de Cuiabá - UNIC

Abstract- In the wake of climate change, cities need to adapt to global warming. In this context, the use of afforestation to improve the microclimate may assist in raising the quality of life for population. This objective requires research that analyzes how the variations in parameters related to canopy dynamics, such as the leaf area index (LAI) and photosynthetically active radiation (PAR) can influence thermal comfort indices. To contribute to this research, this study measured the air temperature, relative air humidity, PAR, and LAI on a monthly basis from July, 2017, to June, 2018, in an urban park in a tropical region of Brazil. Kriging maps were created for the heat index (HI), and multiple polynomial regression models were adjusted to estimate the HI using PAR and LAI data. After defining the models, positive and negative variations of LAI were tested to observe if any changes in HI occurred. The simulated results showed greater sensitivity to negative variations in LAI, in which a 50% reduction in LAI decreased the HI by 28%, particularly during the dry period.

Keywords: *afforestation; air temperature; mobile transect; photosynthetically active radiation; relative humidity; thermal comfort.*

GJHSS-B Classification: FOR Code: 059999



INFLUENCE OF LEAF AREA INDEX ON THE HEAT INDEX OF A TROPIC URBAN PARK

Strictly as per the compliance and regulations of:



RESEARCH | DIVERSITY | ETHICS

© 2021. Jonathan Willian Zangeski Novais, Danielle Da Silva Batista, Renata Luisa Ferreira, Roberta Daniela de Souza, Thiago Fernandes & Carlo Ralph De Musis. This research/review article is distributed under the terms of the Attribution-NonCommercial-NoDerivatives 4.0 International (CC BY-NC-ND 4.0). You must give appropriate credit to authors and reference this article if parts of the article are reproduced in any manner. Applicable licensing terms are at <https://creativecommons.org/licenses/by-nc-nd/4.0/>.

Influence of Leaf Area Index on the Heat Index of a Tropic Urban Park

Jonathan Willian Zangeski Novais ^α, Danielle Da Silva Batista ^σ, Renata Luisa Ferreira ^ρ,
Roberta Daniela de Souza ^ω, Thiago Fernandes[‡] & Carlo Ralph De Musis[§]

Abstract[†] - In the wake of climate change, cities need to adapt to global warming. In this context, the use of afforestation to improve the microclimate may assist in raising the quality of life for population. This objective requires research that analyzes how the variations in parameters related to canopy dynamics, such as the leaf area index (LAI) and photosynthetically active radiation (PAR) can influence thermal comfort indices. To contribute to this research, this study measured the air temperature, relative air humidity, PAR, and LAI on a monthly basis from July, 2017, to June, 2018, in an urban park in a tropical region of Brazil. Kriging maps were created for the heat index (HI), and multiple polynomial regression models were adjusted to estimate the HI using PAR and LAI data. After defining the models, positive and negative variations of LAI were tested to observe if any changes in HI occurred. The simulated results showed greater sensitivity to negative variations in LAI, in which a 50% reduction in LAI decreased the HI by 28%, particularly during the dry period. As the area is a region that experiences considerable variability in terms of humidity and high temperatures throughout the year, conditions conducive to thermal discomfort had often occurred in the study area. This indicates that for tropical regions, even in urban parks, it is important that users pay close attention to their hydration needs and the duration and intensity of their physical activities.

Keywords: afforestation; air temperature; mobile transect; photosynthetically active radiation; relative humidity; thermal comfort.

1. INTRODUCTION

Climate change and its impacts associated with anthropogenic actions including vegetation suppression, land use, and occupation, and the dense and compact set of constructions from constant urban expansion have become the focus of widespread discussion amongst the scientific community (Grimmond et al., 2009; Middel et al., 2014; Petralli et al., 2014). This is due to the changes in the thermodynamic field caused by the decrease in shortwave reflection and increased emission of long waves; this causes an increase in air temperature even during the periods of shorter heat stroke duration,

Author α: Universidade de Cuiabá – UNIC, Brazil.
e-mail: jonathan.novais@kroton.com.br

[†] Abbreviations: GRG: generalized reduced gradient; HI: heat index; LAI: leaf area index; MODIS: Moderate Resolution Imaging Spectroradiometer; PAR: photosynthetically active radiation; SQDP: sum of squares of weighted deviations; SSR: sum of the squares of residues.

intensifying the formation of heat islands (Ayoade, 2003; Peng et al., 2012).

Artificialized areas, mainly in the central regions of cities, produce greater changes in the local climate. Consequently, vegetated urban spaces contribute to better thermal comfort and the reduction of heat islands. This is because of the interception of a part of the solar radiation incident by the tree canopy; the extent of interception varies based on the species, resulting in differing attenuation of solar radiation. (Abreu et al., 2012). Herb et al. (2008) affirmed that the canopy of trees affects the heat transfer of the surface and the temperature of the soil below it, providing better thermal conditions for pedestrian movement (Souza et al., 2020).

Thus, the variations in leaf area indices (LAI) may influence thermal comfort, especially in tropical regions with seasonal precipitation. According to Llandert (1982), thermal comfort associated with the presence of afforestation is mainly related to the canopy density of each tree. Through its leaves, trees are able to absorb 15% to 35% of the received light energy, pass between 30% and 50% of the energy, and reflects the remainder of the energy (~30% to 40%), during the daytime.

The constant concern on promoting the quality of life in cities and the health of the population has fostered the use of research and different methodologies, to demonstrate the effective action of vegetation on the urban microclimate (Bueno-Bartholomei, 2003; Abreu and Labaki, 2008; Monteiro and Alluci, 2008). Grimmond and Oke (1991) and Krayenhoff et al. (2014) have shown that soil and vegetation can moderate the local microclimate by delaying the release of water through evapotranspiration, reinforcing the importance of urban parks in cities climate. Ren et al. (2013) confirmed that the population recognizes urban parks as an oasis amid the dense urban construction model, acting to alleviate the thermal discomfort of heat islands.

One way to measure a user's comfort index is the heat index (HI) method proposed by Steadman (1979a, 1979b, 1984). This method is one of the most popular environmental health indices, providing the basis for heat warnings in many communities of the United States of America (NOAA, 2009). The heat index has also been applied in several regions and climates in

Brazil. For example, Nóbrega and Verçosa (2011) applied the HI in Recife, a seaside town with an Am climate according to the Köppen classification. Silva and Streck (2014) applied the HI to the Cfa climate in Santa Maria, a southern Brazilian city. Souza et al. (2020) applied the HI to an Aw climate classification to Cuiabá City, a midwest city in Brazil.

In Brazil, although urban parks are common, it is typical to find temperatures close to 40 °C, even in vegetated areas (Maciel et al. 2011; Pacheco et al. 2018; Andrade et al. 2019). This highlights the need to verify the comfort of users of urban parks in tropical

regions and analyze how the LAI may influence thermal comfort. The objective of this study is to analyze the influence of the variations in LAI on the HIs of a tropical urban park.

II. MATERIALS AND METHODS

a) Study area

This research was conducted at the Conservation Unit Ilto Ferreira Coutinho Park, located in the central region of the municipality of Tangará da Serra, state of Mato Grosso, Brazil (Fig. 1).

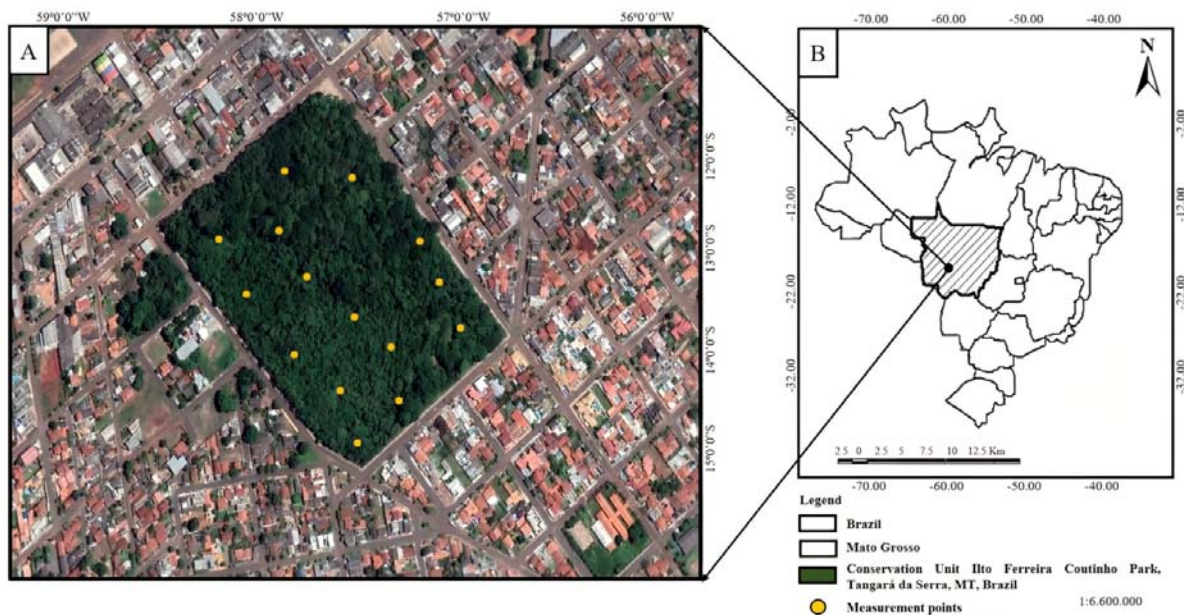


Figure 1: Map of the study area: A) Brazil and Mato Grosso State, B) Conservation Unit Ilto Ferreira Coutinho Park, Tangará da Serra, MT, Brazil.

The study area is located at 14°37'08"S and 57°29'09"W, with an altitude of 452 m and spans approximately 12 ha (Melz and Tiago, 2009). The original growth of semideciduous forest is characterized as Cerrado-Amazonian ecotone. The most abundant families are Anacardiaceae, Malvaceae, Bignoniaceae, Annonaceae, Apocynaceae, Meliaceae, Miristicaceae, and Rubiaceae, where 81% of the species are native to the region (Rodrigues, et al., 2015). There are two types of soils in the study area: red dystrophic latosol (red latosol) and hydromorphic quartzenic neosol. Based on the Köppen climate classification, the climate is Aw which is characterized as hot and humid with rain in the summer and drought in the winter with wet and dry seasons (Alvares et al., 2013). The surroundings are composed of commercial areas and single-story residences, with very little shade generated by buildings.

b) Measurement of Environmental Variables and Study Period

Air temperature and relative humidity were collected for one year, on a monthly basis, Data

collection commenced in July 2017 and ceased in June 2018, from 8 am to 5 pm, with an hourly collection, at a central park point; the averages were subsequently calculated. Collection days were preferentially chosen when there was no rain or cloud, based on the method described in Oke (1982). Measurements were obtained using a portable microclimate station (Kestrel 4500 Weather Tracker, NK Company, Boothwyn, PA, USA).

The incident photosynthetically active radiation (PAR) data and LAI were collected at 12 pm at 15 points distributed throughout the park; the averages of these values were calculated following the measurement. This data was measured using a linear ceptometer (AccuPar - LP 80, Decagon Devices, Washington, USA).

The mobile transect method was used for geostatistical analysis, with air temperature and relative humidity data collected every minute during a trip that covered all regions of the park. The collections were made at 8am, 12am, and 5pm, in January and June 2018, to cover the seasonality of the region. The HI was calculated based on these results, and the semi-variograms and kriging map were obtained. Data was

collected at a height of approximately 1 m from the ground, according to the guidelines in Ferreira et al. (2015), França et al. (2016), Porangaba and Amorim (2017), França et al. (2018), and Alves et al. (2019). Because the sensor is open path, not aspirated, it was also important that measurements occurred when the air was not completely stagnant during the study to minimize lags in sensor response (Sun, 2011).

The HI was proposed by Steadman (1979a), according to Equation (1):

$$HI = -42,379 + 2,049015230 \cdot T_{air} + 10,14333127 \cdot R_h - 0,22475541 \cdot T_{air} \cdot R_h - 6,83783 \cdot 10^{-3} \cdot (T_{air})^2 - 5,481717 \cdot 10^{-2} \cdot (R_h)^2 + 1,22874 \cdot 10^{-3} \cdot (T_{air})^2 \cdot R_h + 8,5282 \cdot 10^{-4} \cdot T_{air} \cdot (R_h)^2 - 1,99 \cdot 10^{-6} \cdot (T_{air})^2 \cdot (R_h)^2 \quad (1)$$

where HI is the heat index (°F), T_{air} is the actual air temperature (dry bulb temperature) (°F), and R_h is relative humidity (%). The data in °F was subsequently converted to °C.

The HI results were analyzed according to alert levels detailed in Table 1.

Table 1: Alert level and description of possible physiological consequences to the human body according to the heat index (HI).

Alert level	Heat index (HI)		Symptoms
	°F	°C	
No warning	< 80	< 27	No problem.
Caution	80–90	27-32	Possible fatigue in cases of prolonged exposure and physical activity.
Extreme caution	90–105	32–41	Possible cramps, sunstroke, and exhaustion due to prolonged exposure and physical activity.
Danger	105-130	41–54	Cramps, sunstroke, and likely exhaustion. Possible brain damage due to prolonged exposure to physical activity.
Extreme danger	> 130	> 54	Stroke or action and risk of imminent cerebral vascular accident.

Source: Adapted from the National Weather Service Weather Forecast Office, NOAA.

d) Statistical Analysis

The T-test test was used to verify possible statistically significant differences to air temperature, relative humidity, and HI, at a significance level of 5%. This was carried out to verify possible differences between the periods, and the Pearson's correlation was used to identify dependencies between meteorological variables.

For spatial analysis, semi-variograms were adjusted to the results of the HI. The semi-variance measures the degree of dependence between two samples. It increases as the distance between points increases, until it stabilizes at the point known as the threshold ($C_0 + C_1$), with half the hope of variance between the pairs of points separated by a distance "h" represented by the classic model, according to Equation (2) as follows:

$$\gamma(h) = \frac{1}{2N(h)} \sum_{i=1}^{N(h)} [Z(x_i) - Z(x_i + h)]^2 \quad (2)$$

Where $\gamma(h)$ is the estimator of semi-variance for each distance, h; $N(h)$ is the number of pairs of points separated by the distance, h; $Z(x)$ is the regionalized

c) Heat index

The HI was calculated for thermal comfort analysis, often used for hot regions with low-intensity winds and where an individual is in the shade. This results in the body thermal sensation based on the air temperature and relative humidity (Steadman, 1979b).

variable at point, x; and $Z(x+h)$ is the value of point $x+h$ (Burrough and Macdonnell, 1998). The semi-variogram is represented by the plot of h versus h. The theoretical semi-variogram generated by this function must be adjusted with a theoretical model that provides the parameters nugget effect (C_0), sill ($C_0 + C_1$), and range (A_0). The degree of spatial dependence of variables was classified according to Cambardella et al. (1994); there was strong spatial dependence when semi-variograms had a nugget effect that was 25% from the threshold, moderate when between 25 and 75%, and weak when greater than 75%.

The theoretical semi-variogram models consisted of spherical, exponential, and Gaussian models described by Andriotti (2003) and Yakamoto and Landim (2013). These models were used to estimate the semi-variance at any distance between samples using the developed GS + (GS +, 2000) software by Gamma Design Software and spreadsheets. The selection of most optimal semi-variogram adjustment method was important as this is the reference point from which the spatial correlation



structure to be used in the inferential kriging procedure is interpreted (Dias et al., 2015).

The evaluation and selection of most optimal adjustments of experimental semi-variograms were based on the smallest sum of the squares of weighted deviations (SQDP) and the highest coefficient of determination (R^2 ; Andriotti, 2003; Yakamoto and Landim, 2013). The interpolation and spatialization of the variables were then carried out using the punctual ordinary kriging; their spatial distribution was subsequently analyzed.

For models estimating the HI as a function of PAR and LAI, the multiple polynomial regression method

was applied, using the Solver tool of Microsoft Excel®. This tool uses the generalized reduced gradient (GRG) as the solution method, adjusting five parameters (A, B, C, D, and E) as per Equation (3):

$$HI_{mod} = (A * LAI^B) + (C * PAR^D) + E \quad (3)$$

After determining the adjusted equation, a t-test was conducted to compare the calculated and modeled data. The LAI was varied positively and negatively by 10%, 20%, 30%, 40%, and 50%, to enable projections on how LAI variation may interfere with HI.

III. RESULTS

a) Hourly and Seasonal Analyses

Hourly averages were determined for air temperature, relative humidity, and HI data for mobile transects conducted in dry and rainy periods, as shown in Fig. 2.

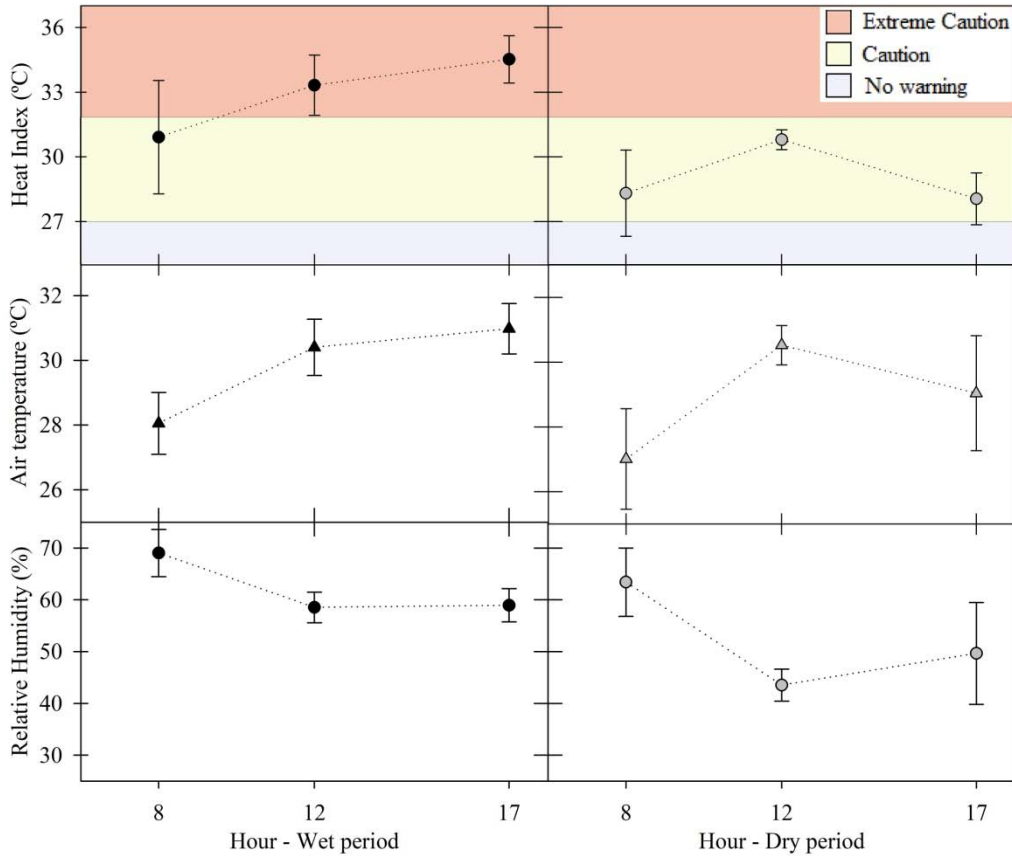


Figure 2: Hourly averages and standard variation for data on heat index, air temperature, and relative air humidity for urban park transects for wet and dry periods.

For the wet season, 12 h and 17 h were classified as “Extreme Caution”, according Table 1, and 8 h as “Caution”. The greatest discomfort observed occurred at sunset at 17 h, reaching 34.52 ± 1.09 °C.

The wet season is the period has the highest incidence of solar radiation, as it is summer in the Southern Hemisphere; this equates to higher temperatures and relative humidity. During the dry period, the average

temperatures over the three measurements throughout the day were always within the “Caution” classification.

Possible edge effects may contribute to the greatest standard deviations observed in during the mornings; this was a variation of 2.62 °C for the wet season and 1.99 °C for the dry season. The regions outside the park were observed to heat up relatively rapidly due to the specific heat of the building materials. This was an occurrence that had been attenuated during other times as the park heats up.

For seasonality analysis, the difference in median values between the two groups for air temperature, relative humidity, and HI was greater than expected, a statistically significant difference was observed ($P < 0.001$). Thus, the seasonality results follow local weather patterns.

Spatial analyses were conducted to observe the distribution of the HI in the park and possible edge effects. For this purpose, semi-variograms were calculated according to Table 2.

Table 2: Adjustment of semivariograms for heat index: model, nugget effect (C_0), sill ($C_0 + C$), range (A_0), determination coefficient (R^2), and sum of squares of residuals (SSR) and spatial relationship.

	Wet			Dry		
	8am	12am	17pm	8am	12am	17pm
Model	Spherical	Exponential	Spherical	Spherical	Spherical	Spherical
C_0	0.01	0.57	0.41	0.01	0.10	0.001
$C_0 + C$	8.51	2.56	1.49	4.48	0.35	3.01
A_0	170.5	101.1	227.8	163.8	501.5	295.8
R^2	0.827	0.78	0.89	0.97	0.862	0.939
SQR	13.8	0.527	0.115	0.489	0.001	0.878
$C_0/(C_0 + C)$	0.001	0.222	0.275	0.002	0.29	0.001
	Strong	Strong	Moderate	Strong	Moderate	Strong

The largest nugget effect found (C_0) was 0.57, and relatively small values of the nugget effect indicated minor errors in measurements (Dafonte et al., 2010). With the exception the 12 am measurement during the wet season in which the adjustment was exponential, all other adjustments were spherical. Of the six schedules analyzed, there was a strong spatial dependence in four; according to the classification of Cambardella et al. (1994), there is only strong spatial dependence when the nugget effect is up to 25% of the sill. Moderate dependency occurred twice, between 5 pm during the wet season and 12 am in the dry season.

The greatest range (A_0) occurred at midday in the dry period, with 501.5 m, generating the observed similarity in the special HI, as shown in Fig. 3. The lack of humidity and diminished leaf area accounted for the standardization observed in the dry season, as shown in Table 2 and Fig. 3. The range is of fundamental importance to interpret the semi-variograms, indicating the distance to where sampling points correlate with each other (Carvalho et al., 2002). This ensures that all neighboring points are so similar that they may be used to estimate values for any point between them (Machado et al., 2007).

The lowest coefficient of determination was 0.78, at 12am during the wet season, suggesting good model adjustments. Regarding the sum of the squares of residues (SSR), only the 8 am measurement during the wet season had values exceeding. As the SSR is a measure of discrepancy between the actual and modeled data, a small SSR indicates a tight fit between the model and the measured data (Draper and Smith, 1998).

The spatial patterns follow the hourly patterns shown in Fig. 2, in which in the spatial analyses of the wet season showed that thermal discomfort was greater in this season than the dry season. Dense vegetation cools the air as it prevents radiation from reaching the forest floor (Napoli et al., 2016) and provides a larger surface area for evaporative cooling. However, the incidence of radiation in the summer season was able to elevate air temperatures, resulting in higher heat levels during the wet season.

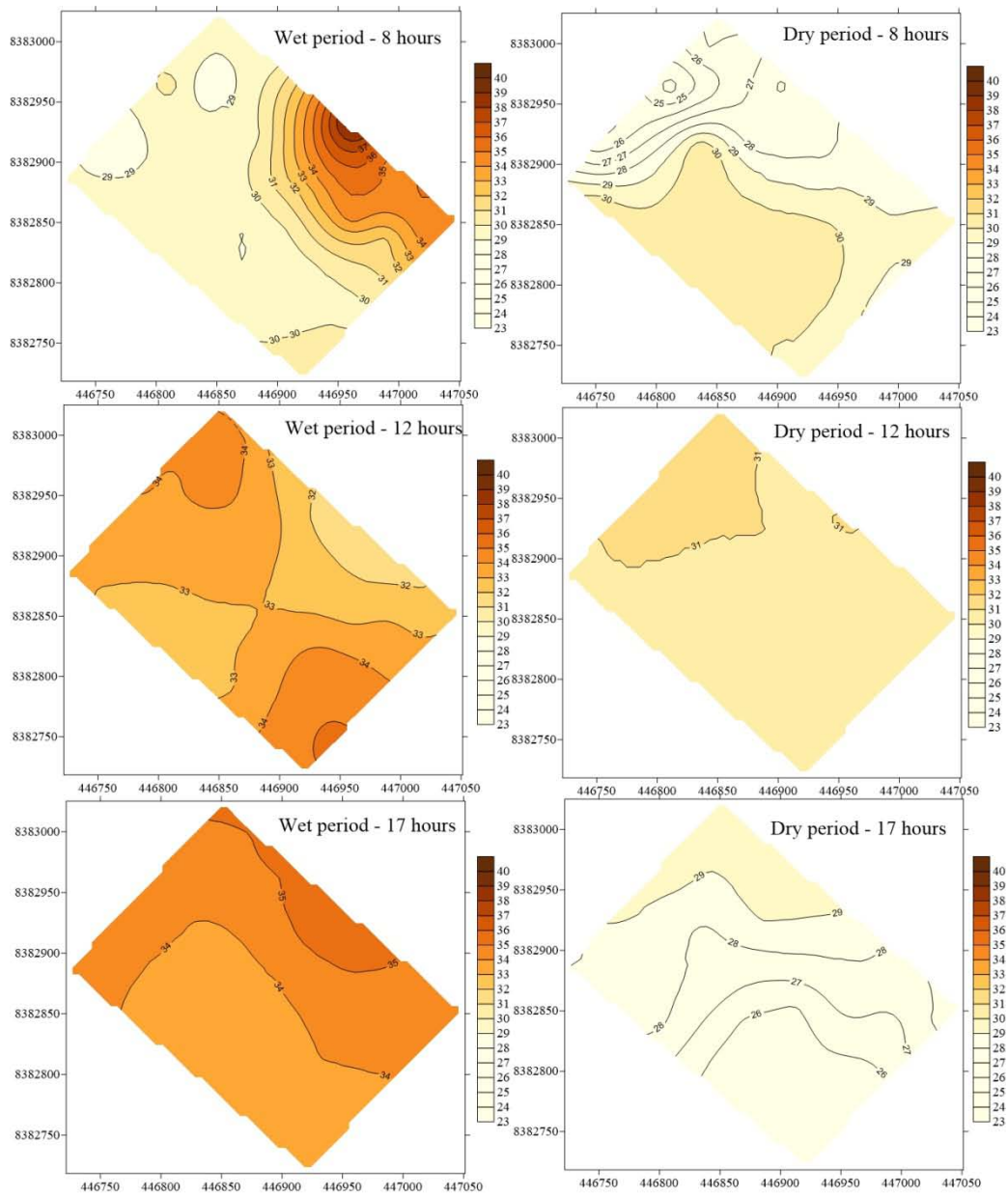


Figure 3: Kriging map for the heat index for times 8, 12, and 17 in the dry and wet periods of the year 2018 for the urban park.

b) Monthly and Model Analysis

Fig. 4 shows the monthly averages of analyzed variables.

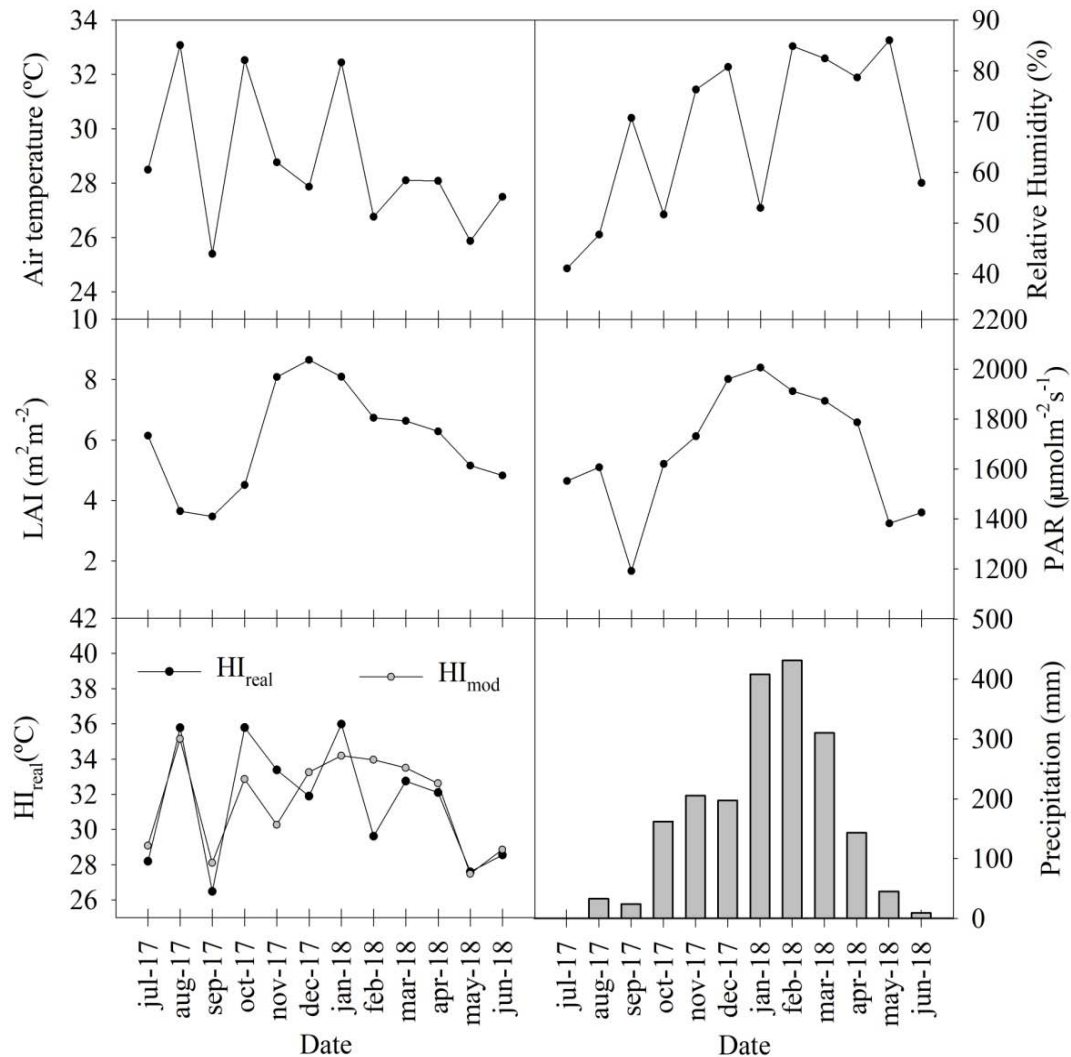


Figure 4: Monthly averages of air temperature, relative air humidity, leaf area index, photosynthetically active radiation, and real and modeled heat index.

According to the Pearson's correlation test (r), air temperature and relative humidity were negatively correlated ($r = -0.666$ and $p > 0.01$). This means that an increase or decrease in air temperature results in an increase or decrease in relative air humidity. Varejão-Silva (2006) explained that such behavior is caused by the inverse proportionality of the relative air humidity and the vapor saturation point. Therefore, the relative air humidity will also be inversely proportional to the air temperature.

The annual average LAI was approximately $6 \text{ m}^2\text{m}^{-2}$, demonstrating regional seasonality. These values are close to those reported by Sanches et al. (2008) who used the Moderate Resolution Imaging Spectroradiometer (MODIS) satellite and reported values between 5.25 to $5.54 \text{ m}^2\text{m}^{-2}$ for another area of the Cerrado-Amazonian ecotone forest. As the urban

park vegetation is a seasonal semi-deciduous forest, leaf loss occurs from August onwards, decreasing the LAI. Another factor that contributes to lower LAI is the solar declination angle; during the dry season this angle is higher (Spolador et al., 2006; Novai et al., 2018). The greater the zenith angle, the greater the path traveled by radiation within the canopy, increasing the chance of absorption by leaves and branches (Senna et al., 2005), this increase is associated due to the measurement technique, which uses the linear ceptometer. PAR data followed the radiation pattern of the Southern Hemisphere, according to Novais et al. (2016), and LAI and PAR were strongly correlated ($r = 0.804$ and $p > 0.01$), to the maximum incidence of PAR in January, approximately $2006 \text{ mol m}^2\text{s}^{-1}$.

The accumulated rainfall throughout the analyzed period was 1968 mm ; in July 2017, there was

no rain whereas February was the rainiest with 431 mm, which is approximately 22% of total annual precipitation. The seasonal pattern of precipitation in the study area is in line with the regional forecast as rainfall is concentrated between October and April in the Cerrado region (Dallacort et al., 2011).

Using PAR and LAI data, the following model was obtained for HI estimates:

$$HI_{mod} = (51.63 * LAI^{-1.19}) + (107.57 * PAR^{0.11}) \pm 216.29 \quad (4)$$

The difference between the mean values of HI_{real} and HI_{mod} was insufficient to reject the possibility that this difference was due to random sampling variability. There was no statistically significant difference between the groups ($P = 0.996$), justifying the use of the model to simulate LAI variations.

Table 3 presents the annual averages of the HI for each model variations and their respective differences from the original value.

Table 3: Average annual heat index values for the LAI models.

		0%	10%	20%	30%	40%	50%
HI	LAI +	31.504	30.77	30.17	29.67	29.25	28.89
	LAI -		32.42	33.58	35.11	37.21	40.25
Variation	LAI +	-	-2.34%	-4.24%	-5.83%	-7.17%	-8.32%
	LAI -		2.88%	6.58%	11.44%	18.11%	27.74%

* LAI + corresponds to positive variations in leaf area index and LAI- to negative variations.

The addition of 50% LAI improved the annual average HI by approximately 8.32%, whereas the decrease resulted in a 27.74% decrease in the average

annual HI. Fig. 5 presents the monthly HI results from the model variations according to the LAI.

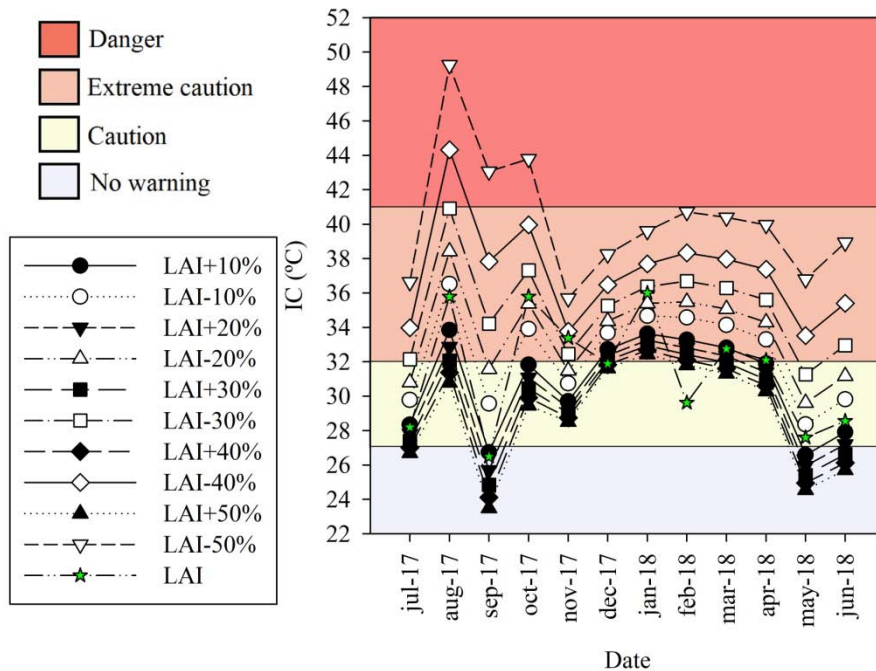


Figure 5: Influence models of leaf area index variation on heat indices.

The 50% variation of LAI showed the most concerning results, where three months were within the "Danger" classification, and the remaining months were in the "Extreme Caution" classification. The positive variations in LAI contributed to a greater number of months in the "No Warning" classification, ranging from zero months in this classification to four months for the LAI +50% model.

IV. DISCUSSION

Based on the analysis of hourly average air temperature and relative humidity generated by the spatialized data, the wet season was more uncomfortable than the dry season. This result differs from the monthly analyses undertaken at a central point of the park. Such differences in results suggest that the spatial patterns of data collection as well as the possible influence of clearings and edges, influenced these

results. These results corroborate the scientific findings from Silva Júnior et al. (2012) for the city of Belém (Pará, Brazil), whereby for the majority of the afternoon the city is thermally uncomfortable. Neighborhoods with a higher percentage of soil sealing and lower vegetation cover exhibited greater thermal discomfort, indicating that urban elements (paved streets, houses, buildings, and vehicle routes), influence the city's climate.

In terms of the influence of the edge effect, Vasconcelos and Zamparoni (2011) and Morakinyo et al. (2017) found that the effectiveness of trees to improve daytime thermal comfort reduces with increasing urban density whereas the opposite was true for the nighttime. Therefore, as the park is not influenced by external shading due to low construction density and people do not visit the park at night, there is no problem using species that have higher LAI, as it is expected that only daytime comfort occurs. This highlights the importance of urban planning to present solutions to promote quality of life within a healthy environment.

The most uncomfortable time was at 5 pm during the wet season, suggesting that despite the high LAI of this period, which mitigates the incidence of solar radiation, air exchange is reduced, making heat dissipation difficult. The cooling effect of vegetation is likely to be lower at night when there is very little transpiration. This means less evaporative cooling (Richards et al., 2020) because of the trapped heat and humidity within the urban canopy layer, compared with the rapid nocturnal cooling of open areas (Fahmy et al. 2010). Boone (2008) explains that humidity often creates a temperature that feels hotter than reality. This is because the body cools with the evaporation of sweat due to the consumption of latent heat on the surface of the skin. However, when air humidity rises, there is a decrease in the rate of sweat evaporation, causing greater heat retention and leading to discomfort and stress (Delworth et al., 1999).

In terms of the analysis of monthly averages, the temperature decreases in September (the dry season), may be related to cold fronts, where there are sharp drops in solar incidence due to the presence of cloudiness (Biudes et al., 2015).

For model analysis, the annual average LAI was approximately $6 \text{ m}^2\text{m}^{-2}$; this is a relatively high value compared to cerrado forests, where Hoffman et al. (2005) found an annual average of $3.3 \text{ m}^2\text{m}^{-2}$ for grassland and $4.2 \text{ m}^2\text{m}^{-2}$ for riparian forest. Malhado et al. (2015) calculated an average annual LAI of $5.07 \text{ m}^2\text{m}^{-2}$, which was closer to Amazonian forest values.

Thus, whilst dense canopy does contribute to thermal comfort, its contribution is not as great as the decrease in LAI, which leads to greater variations in HI, making the HI reach $40.25 \text{ }^\circ\text{C}$ (extreme Caution Alert Level); this constitutes a $\sim 28\%$ increase in relation to measured values.

Despite the general consensus that urban parks are the places of leisure and exercise as well as oases within the urban area, in tropical areas, greater attention should be given to vulnerable users of the park, for instance, those susceptible to cramps, sunstroke and likely exhaustion, and possible brain damage due to prolonged exposure to more intense physical activities. This is because the heat indices during the dry season was largely unsatisfactory.

V. CONCLUSION

The LAI influences the HI, and this influence is more pronounced in models that decrease the amount of leaves. A 50% reduction in LAI caused a 28% increase in the HI, being classified as "Extreme Caution" alert level during the dry season which was found to be more susceptible to the changes in the LAI. Hourly analysis showed that the evening, especially in the wet season, was of greater concern, as there was a lack of thermal comfort even in shaded areas. The possible nighttime discomfort generated by the heat retained in the park is insufficient to cause major concern, as park visit is typically limited to the daytime. Although urban parks are recognized as a place for leisure and physical activities, greater care is suggested during the use of urban parks in tropical regions. It is recommended that park users equip themselves with light clothing, hydration, and are careful with strenuous activities, avoiding the periods of greatest thermal discomfort.

Funding

This work was supported by the Mato Grosso Research Support Foundation-FAPEMAT [grant number 0194288/2017].

REFERENCES RÉFÉRENCES REFERENCIAS

1. Abreu, L. V., & Labaki, L. C. (2008). Avaliação da Termo-Regulação em Diferentes Espécies Arbóreas. *ENCONTRO NACIONAL DE TECNOLOGIA DO AMBIENTE CONSTRUÍDO*, 12.
2. Abreu-Harbach, L.V, Labaki, L.C, & Matzarakis, A. (2014). Bioclima térmico como fator de planejamento urbano e arquitetônico em climas tropicais - o caso de Campinas, Brasil. *Urban Ecosystems*, 17 (2), 489-500. *Doi*: 10.1007/s00704-013-0886-0
3. Alvares, C. A., Ji, S., & Sentelhas, P. C. gONÇAlVeS JIM AND SPAROVeK, g. 2013. Köppen's climate classification map for Brazil. *Metereol*, (22), 6. *Doi*: 10.1127/0941-2948/2013/0507.
4. Alves, A. C. M., Nogueira, M. C. D. J. A., de Moura Santos, F. M., de Muis, C. R., & de Souza Nogueira, J. (2019). Impacto da morfologia de parque urbano no microclima e no conforto térmico de Cuiabá-Brasil. *Revista Brasileira de*

- Climatologia*, 24, Doi: <http://dx.doi.org/10.5380/abclima.v24i0.58644>
5. Andrade, L. P., Nogueira, M. C. J. A., Santos, F. M. M., Nogueira, J. S., Musis, C. R., Novais, J, W. Z. (2019). Atmospheric Pollution and Meteorological Parameters in the City of Cuiabá-MT. *Modern Environmental Science and Engineering*. 5(6), 474-481. Doi: 10.15341/mese(2333-2581)/06.05.2019/003.
 6. Andriotti, J. L. S. (2003). *Fundamentos de estatística e geoestatística* (No. 551: 519.2 AND).
 7. Ayoadé, J. O. (2007). Introdução à Climatologia para os Trópicos. 11ª edição. Editora Bertrand Brasil, Rio de Janeiro.
 8. Biudes, M. S., Vourlitis, G. L., Machado, N. G., de Arruda, P. H. Z., Neves, G. A. R., de Almeida Lobo, F., ... & de Souza Nogueira, J. (2015). Patterns of energy exchange for tropical ecosystems across a climate gradient in Mato Grosso, Brazil. *Agricultural and Forest Meteorology*, 202, 112-124. Doi: 10.1016/j.agrformet.2014.12.008.
 9. Bartholomei, C. L. B. (2003). Influência da vegetação no conforto térmico urbano e no ambiente construído.
 10. Burrough, P. A., McDonnell, R., McDonnell, R. A., & Lloyd, C. D. (2015). *Principles of geographical information systems*. Oxford university press.
 11. Cambardella, C. A., Moorman, T. B., Novak, J. M., Parkin, T. B., Karlen, D. L., Turco, R. F., & Konopka, A. E. (1994). Field-scale variability of soil properties in central Iowa soils. *Soil science society of America journal*, 58(5), 1501-1511. Doi: 10.2136/sssaj1994.03615995005800050033x.
 12. Carvalho, J. R. P. D., Silveira, P. M. D., & Vieira, S. R. (2002). Geoestatística na determinação da variabilidade espacial de características químicas do solo sob diferentes preparos. *Pesquisa Agropecuária Brasileira*, 37(8), 1151-1159. Doi: 10.1590/S0100-204X2002000800013.
 13. Dafonte, J. D., Guitián, M. U., Paz-Ferreiro, J., Siqueira, G. M., & Vázquez, E. V. (2010). Mapping of soil micronutrients in an European Atlantic agricultural landscape using ordinary kriging and indicator approach. *Bragantia*, 69, 175-186. Doi: doi.org/10.1590/S0006-87052010000500018.
 14. Dallacort, R., Martins, J. A., Inoue, M. H., de Freitas, P. S. L., & Coletti, A. J. (2011). Distribuição das chuvas no município de Tangará da Serra, médio norte do Estado de Mato Grosso, Brasil. *Acta Scientiarum. Agronomy*, 33(2), 193-200. Doi: 10.4025/actasciagron.v33i2.5838.
 15. Rezende Maciel, C., Nogueira, M. C. D. J. A., & de Souza Nogueira, J. (2011). Ground cover and its influence on temperature of urban microclimate of Cuiabá-MT. *Caminhos de Geografia*, 12(39).
 16. Dias, M. V. R., de Carvalho Alves, M., & Sanches, L. (2015). Métodos de ajuste de semivariogramas para modelagem espacial de íons de precipitação pluvial em Cuiabá, Brasil. *Ciência e Natura*, 37(2), 312-320. Doi: 10.5902/2179460X12101.
 17. Draper, N. R., & Smith, H. (1998). Análise de regressão aplicada.
 18. Fahmy, M., Sharples, S., & Yahiya, M. (2010). LAI based trees selection for mid latitude urban developments: A microclimatic study in Cairo, Egypt. *Building and Environment*, 45(2), 345-357. Doi: <https://doi.org/10.1016/j.buildenv.2009.06.014>.
 19. Ferreira, L., Carrilho, S. T., & Mendes, P. C. (2015). Áreas verdes urbanas: uma contribuição aos estudos das ilhas de frescor. *Brazilian Geographical Journal: geosciences and humanities research medium*, 6(2), 101-120.
 20. França, M. S., de França, S. M. B., Nogueira, M. C. D. J. A., & de Souza Nogueira, J. (2016). Estimativa do conforto térmico na cidade de Cuiabá/MT. *Revista de Ciências Ambientais*, 10(1), 59-73. Doi: <http://dx.doi.org/10.18316/1981-8858.16.22>
 21. França, M. S. (2018). Estimativa de índices de conforto térmico por meio do uso de transecto móvel em Sorriso/MT. *Revista Nativa*, Sinop-MT, 6(6), 648-653. Doi: <http://dx.doi.org/10.31413/nativa.v6i6.5820>
 22. Grimmond, C. S. B., Best, M., Barlow, J., Arnfield, A. J., Baik, J. J., Baklanov, A., ... & Clark, P. (2009). Urban surface energy balance models: model characteristics and methodology for a comparison study. In *Meteorological and Air Quality Models for Urban Areas* (pp. 97-123). Springer, Berlin, Heidelberg. Doi: 10.1007/978-3-642-00298-4_11.
 23. Grimmond, C.S.B., and T.R. Oke. (1991). An evaporation-interception model for urban areas. *Water Resour. Res.* 27:1739-1755. Doi: 10.1029/91WR00557
 24. Hoffmann, W. A., da Silva, E. R., Machado, G. C., Bucci, S. J., Scholz, F. G., Goldstein, G., & Meinzer, F. C. (2005). Seasonal leaf dynamics across a tree density gradient in a Brazilian savanna. *Oecologia*, 145(2), 306-315. Doi: 10.1007/s00442-005-0129-x.
 25. Herb, WR, Janke, B., Mohseni, O., & Stefan, HG (2008). Simulação da temperatura da superfície do solo para diferentes coberturas do solo. *Journal of Hydrology*, 356 (3-4), 327-343. Doi: 10.1016/j.jhydrol.2008.04.020.
 26. Junior, J. D. A. S., Costa, A. C. L., Pezzuti, J. C. B., Costa, R. F., & Galbraith, D. (2012). Análise da distribuição espacial do conforto térmico da cidade de Belém, PA no período menos chuvoso. *Revista Brasileira de Geografia Física*, 5(2), 218-232. Doi: 10.26848/rbgf.v5.2.p218-232.
 27. Krayenhoff, E.S., A. Christen, A. Martilli, and T.R. Oke. (2014). A multi-layer radiation model for urban neighbourhoods with trees. *Boundary-Layer*

- Meteorol. 151:139–178. *Doi:* 10.1007/s10546-013-9883-1
28. Machado, N. G., Sanches, L., Silva, L. B., Novais, J. W. Z., Aquino, A. M., Biudes, M. S., ... & Nogueira, J. S. (2015). Soil nutrients and vegetation structure in a neotropical seasonal wetland. *Applied ecology and environmental research*, 13(1), 289-305. *Doi:* 10.15666/aeer/1302_289305.
 29. Malhado, A. C., Costa, M. H., de Lima, F. Z., Portilho, K. C., & Figueiredo, D. N. (2009). Seasonal leaf dynamics in an Amazonian tropical forest. *Forest ecology and management*, 258(7), 1161-1165. *Doi:* <https://doi.org/10.1016/j.foreco.2009.06.002>
 30. Marimon, B. S., Lima, E. D. S., Duarte, T. G., Chieregatto, L. C., & Ratter, J. A. (2006). OBSERVATIONS ON THE VEGETATION OF NORTHEASTERN MATO GROSSO, BRAZIL. IV. AN ANALYSIS OF THE CERRADO-AMAZONIAN FOREST ECOTONE; THE CERRADO-AMAZONIAN FOREST ECOTONE IN BRAZIL; BS MARIMON ET AL. *Edinburgh Journal of Botany*, 63(2-3), 323. *Doi:* <https://doi.org/10.1017/S0960428606000576>
 31. Melz, E. M., & Tiago, P. V. (2009). Propriedades físico-químicas e microbiológicas do solo de um Parque em Tangará da Serra, MT, uma área de transição entre Amazônia e Cerrado. *Acta Amazonica*, 39(4), 829-834. *Doi:* 10.1590/S0044-59672009000400011.
 32. Middel, A., Hüb, K., Brazel, A. J., Martin, C. A., & Guhathakurta, S. (2014). Impact of urban form and design on mid-afternoon microclimate in Phoenix Local Climate Zones. *Landscape and Urban Planning*, 122, 16-28. *Doi:* 10.1016/j.landurbplan.2013.11.004.
 33. Monteiro, L. M., & Alucci, M. P. (2008). Modelos Preditivos de Estresse Termo-Fisiológico: estudo empírico comparativo em ambientes externos. *ENCONTRO NACIONAL DE TECNOLOGIA NO AMBIENTE CONSTRUÍDO*, 12.
 34. Morakinyo, T. E., Kong, L., Lau, K. K. L., Yuan, C., & Ng, E. (2017). A study on the impact of shadow-cast and tree species on in-canyon and neighborhood's thermal comfort. *Building and Environment*, 115, 1-17. *Doi:* 10.1016/j.buildenv.2017.01.005.
 35. Napoli, M., Massetti, L., Brandani, G., Petralli, M., & Orlandini, S. (2016). Modeling tree shade effect on urban ground surface temperature. *Journal of environmental quality*, 45(1), 146-156. *Doi:* 10.2134/jeq2015.02.0097.
 36. NOAA (National Oceanic and Atmospheric Administration). (2009). National Weather Service Glossary. Available: <http://w1.weather.gov/glossary/> [accessed 12 August 2020].
 37. Nóbrega, R. S., & Verçosa, T. (2011). O microclima e o (des) conforto térmico em ambientes abertos na cidade do Recife. *Revista de Geografia (Recife)*, 28(1), 93-109.
 38. Novais, J. W. Z., Sanches, L., Silva, L. B. D., Machado, N. G., Aquino, A. M., & Pinto Junior, O. B. (2016). Albedo do Solo abaixo do Dossel em Área de *Vochysia divergens* Pohl no Norte do Pantanal. *Revista Brasileira de Meteorologia*, 31(2), 157-166. *Doi:* 10.1590/0102-778631220150001.
 39. Novais, J. W. Z., Sanches, L., Dias, V. R. D. M., Machado, N. G., Silva, L. B. D., & Aquino, A. M. (2018). Space-temporal variation of PAR reflected by the soil and transmitted by the canopy in a floodplain forest of Mato Grosso State, Brazil. *Ciencia Florestal*, 28(4), 1502-1513. *Doi:* 10.5902/1980509835097.
 40. Oke, T. R. (1982). The energetic basis of the urban heat island. *Quarterly Journal of the Royal Meteorological Society*, 108(455), 1-24. *Doi:* 10.1002/qj.49710845502.
 41. Peng, S., Piao, S., Ciais, P., Friedlingstein, P., Oettle, C., Bréon, F. M., ... & Myneni, R. B. (2012). Surface urban heat island across 419 global big cities. *Environmental science & technology*, 46(2), 696-703. *Doi:* 10.1021/es2030438.
 42. Pereira, S. P., Novais, J. W. Z., Júnior, O. B. P., de Musis, C. R., de Andrade, L. P., Joaquim, T. D. O., & Pierangeli, M. A. (2018). Temporal dynamic of CO₂ efflux in a savanna fragment in Mato Grosso. *Revista Ibero-Americana de Ciências Ambientais*, 9(2), 31-40. *Doi:* 10.6008/CBPC2179-6858. 2018.002.0004.
 43. Petralli, M., Massetti, L., Brandani, G., & Orlandini, S. (2014). Urban planning indicators: useful tools to measure the effect of urbanization and vegetation on summer air temperatures. *International Journal of Climatology*, 34(4), 1236-1244. *Doi:* 10.1002/joc.3760.
 44. Porangaba, G. F. O., Amorim, M. C. C. T. (2017). Análise de ilhas de calor diagnosticadas por meio de transectos móveis em Assis, Cândido Mota, Maracá e Tarumã (SP). *Confins. Revue franco-brésilienne de Géographie*, 33(12), 02-15. *Doi:* 10.4000/confins.12729.
 45. Ren, Z., He, X., Zheng, H., Zhang, D., Yu, X., Shen, G., & Guo, R. (2013). Estimation of the relationship between urban park characteristics and park cool island intensity by remote sensing data and field measurement. *Forests*, 4(4), 868-886. *Doi:* 10.3390/f4040868.
 46. Richards, D. R., Fung, T. K., Belcher, R. N., & Edwards, P. J. (2020). Differential air temperature cooling performance of urban vegetation types in the tropics. *Urban Forestry & Urban Greening*, 126651. *Doi:* 10.1016/j.ufug.2020.126651
 47. Rodríguez-Avial Llardent, L. (1982). Zonas verdes y espacios libres en la ciudad. *Instituto de estudios de administración local. Madrid*.

48. Rodrigues, P.P.; Gomes, I.T.S.; Simon, M.L.S.; Nunes, J.R.S.; Añez, R.B.(2015). Inventário florístico no entorno das trilhas do parque natural municipal "Ilto Ferreira Coutinho". Anais: Resumos Expandidos. Vi Simpósio Da Amazônia Meridional Em Ciências Ambientais Scientific Electronic Archives, Special Edition. Vol. 8 (3).
49. Sanches, L., de Andrade, N. L. R., de Souza Nogueira, J., Biudes, M. S., & Vourlitis, G. L. (2008). Índice de área foliar em floresta de transição amazonia cerrado em diferentes métodos de estimativa. *Ciência e Natura*, 30(1), 57-69. Doi: 10.5902/2179460X9750.
50. Senna, M.C, Costa, M.H Shimabukuro, & Y.E. (2005). Fração de radiação fotossinteticamente ativa absorvida pela floresta tropical amazônica: Uma comparação de medições de campo, modelagem e sensoriamento remoto. *Journal of Geophysical Research: Biogeosciences*, 110 (G1).
51. Silva, S. D., & Streck, N. A. (2014). Tendências das séries históricas do índice de calor no município de Santa Maria-RS. *Ciência Rural*, 44(8), 1360-1366. Doi: 10.1590/0103-8478cr20131345.
52. Souza, R. D., Novais, J. W. Z., Pierangeli, M. A. P., Lansanova, M. D., Fernandes, T., Hoki, V. S. P., & Souza, P. J. (2020). Urban microclimate in vegetated and non-vegetated areas in rainy and sunny conditions. *Raega-O Espaço Geográfico em Análise*, 47(1), 136-149. Doi: 10.5380/raega.
53. Spolador, J., Sanches, L., & Costa, M. H. (2006). Radiação fotossinteticamente ativa em uma floresta de transição Cerrado-Amazônica. *Revista Brasileira de Meteorologia*, 21(3b), 301-307.
54. Steadman, R. G. (1979). The assessment of sultriness. Part I: A temperature-humidity index based on human physiology and clothing science. *Journal of applied meteorology*, 18(7), 861-873. Doi: 10.1175/1520-0450(1979)018<0861:T AOSPI>2.0.C O;2
55. Steadman, R. G. (1979). The assessment of sultriness. Part II: effects of wind, extra radiation and barometric pressure on apparent temperature. *Journal of Applied Meteorology*, 18(7), 874-885. Doi: 10.1175/1520-0450(1979)018<0874:TAOSPI>2.0. CO;2
56. Sun, C. Y. (2011). A street thermal environment study in summer by the mobile transect technique. *Theoretical and applied climatology*, 106 (3-4), 433-442. Doi: 10.1007/s00704-011-0444-6.
57. Varejão-Silva, M. A. (2006). Meteorologia e climatologia: versão digital 2. Recife: Esalq.
58. Vasconcelos, L. C., & Zamparoni, C. A. G. P. (2011). Os efeitos da urbanização no microclima no bairro Morada da Serra, Cuiabá-MT. *Raega-O Espaço Geográfico em Análise*, 23, Doi: <http://dx.doi.org/10.5380/raega.v23i0.24922>
59. Yakamoto, J., & Landim, P. (2013). Geoestatística: Conceitos e Aplicações. 1ª Edição. São Paulo: Oficina de Textos.